ORGANIC
LETTERS

2011
Vol. 13, No. 3
490−493

Spontaneous and Selective CO_2 Sorption under Ambient Conditions in Seemingly Nonporous Molecular Crystal of Azacalix[5]arene Pentamethyl Ether

Hirohito Tsue,* Kohei Ono, Satoshi Tokita, Koichi Ishibashi, Kazuhiro Matsui, Hiroki Takahashi, Kazuyuki Miyata, Daisuke Takahashi, and Rui Tamura

Graduate School of Human and Environmental Studies, Kyoto University,
Yoshida-nihonmatsu, Sakyo-ku, Kyoto 606-8501, Japan

tsue@ger.mbox.media.kyoto-u.ac.jp

Received November 22, 2010

ABSTRACT

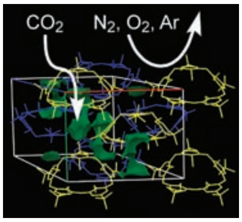

Described are the syntheses, crystal structures, and solid−gas adsorption behaviors of azacalix[4]arene tetramethyl ether and azacalix[5]arene pentamethyl ether. While the former compound exhibited no adsorption of four main atmospheric components, the latter selectively and rapidly adsorbed CO_2 at ambient temperature and pressure. X-ray crystallographic and potential energy distribution analysis revealed that azacalix[5]arene created an energetically favorable space for CO_2 in its seemingly nonporous crystal, leading to the observed selective CO_2 uptake under ambient conditions.

Carbon dioxide is a significant greenhouse gas implicated in global warming. Consequently, the development of new methods for capturing CO_2 is an increasingly important research area since the International Energy Agency claimed the need for more energy efficient and less costly CO_2 capture technologies.[1] At present, the most widely used technology for capturing CO_2 from flue gas is absorption using amine solvents. The major drawback of the amine-based processes is high energy demands to recover the amines for recycling, together with the adverse health and environmental effects caused by the loss of volatile amines. Therefore, numerous studies have thus far explored methods of physisorption on solids because of their low energy requirements and low environmental impacts. Porous materials such as activated carbons,[2] zeolites,[2,3] cucurbiturils,[4] dipeptides,[5] phosphazene,[6] metal−organic frameworks (MOFs),[2,7] and covalent organic frameworks[8] were extensively studied in addition to seemingly nonporous crystals of calixarenes,[9] clarithromicin,[10] metalocycle,[11] and cage-type compounds.[12] Except for a few materials,[3,4b,7] however, selective CO_2 capture particularly at ambient temperature and atmospheric pressure still remains as a major challenge.

---

[1] http://www.iea.org/textbase/nppdf/free/2004/prospects.pdf.

[2] Selected reviews on CO_2 capture by activated carbons, zeolites, and MOFs: (a) Bonenfant, D.; Kharoune, M.; Niquette, P.; Mimeault, M.; Hausler, R. *Sci. Technol. Adv. Mater.* **2008**, *9*, 013007. (b) Horike, S.; Shimomura, S.; Kitagawa, S. *Nat. Chem.* **2009**, *1*, 695–704. (c) Choi, S.; Drese, J. H.; Jones, C. W. *ChemSusChem* **2009**, *2*, 796–854. (d) D'Alessandro, D. M.; Smit, B.; Long, J. R. *Angew. Chem., Int. Ed.* **2010**, *49*, 6058–6082.

[3] (a) Dunne, J. A.; Rao, M.; Sircar, S.; Gorte, R. J.; Myers, A. L. *Langmuir* **1996**, *12*, 5896–5904. (b) Siriwardane, R. V.; Shen, M.-S.; Fischer, E. P.; Poston, J. A. *Energy Fuels* **2001**, *15*, 279–284. (c) Akten, E. D.; Siriwardane, R.; Sholl, D. S. *Energy Fuels* **2003**, *17*, 977–983.

[4] (a) Miyahara, Y.; Abe, K.; Inazu, T. *Angew. Chem., Int. Ed.* **2002**, *41*, 3020–3023. (b) Kim, H.; Kim, Y.; Yoon, M.; Lim, S.; Park, S. M.; Seo, G.; Kim, K. *J. Am. Chem. Soc.* **2010**, *132*, 12200–12202.

[5] Comotti, A.; Bracco, S.; Distefano, G.; Sozzani, P. *Chem. Commun.* **2009**, 284–286.

[6] Sozzani, P.; Bracco, S.; Comotti, A.; Ferretti, L.; Simonutti, R. *Angew. Chem., Int. Ed.* **2005**, *44*, 1816–1820.

10.1021/ol102829h © 2011 American Chemical Society
Published on Web 12/21/2010

We anticipate that a nitrogen-bridged calixarene analogue (azacalixarene)[13] is a good candidate for efficiently capturing CO_2 because the bridging nitrogen atoms can act as conjugation sites with the aromatic rings to establish electron-rich π-systems, thereby boosting intermolecular interactions with CO_2 having large polarizability and a large quadrupole moment. Indeed, we previously observed that, although azacalix[4]arene **1** exhibited no CO_2 uptake, azacalixarenes **4** and **5** selectively adsorbed CO_2 at ambient pressure among four main atmospheric components such as N_2, O_2, Ar, and CO_2.[14] However, a low temperature of 195 K was required as an "external energy" to achieve the effective CO_2 uptake in **4** and **5**. This foregoing finding led us to investigate the solid−gas adsorption behaviors of the smaller homologues **2** and **3**. From the present study on them, it has been revealed that, while azacalix[4]arene **2** adsorbs no CO_2 as in the case of the *N*-methylated derivative **1**,[14a] azacalix[5]arene **3** exhibits spontaneous and selective CO_2 capture at ambient temperature and pressure.[15] In this paper, we report the syntheses, crystal structures, and gas adsorption behaviors of **2** and **3**.

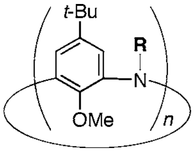

1: $n = 4$, **R** = Me
2: $n = 4$, **R** = H
3: $n = 5$, **R** = H
4: $n = 6$, **R** = H
5: $n = 7$, **R** = H

Azacalixarenes **2** and **3** were prepared according to Schemes S1 and S2 in the Supporting Information. A single crystal of **2** was obtained by slow crystallization from acetone.[16] X-ray crystallographic analysis revelaed that azacalix[4]arene **2** adopted a 1,3-alternate conformation in the solid state (Figure 1a) and formed a densely packed crystal structure[17] (Figures 1b and S9) similar to that of **1**,[18] though small discrete voids of 66 Å^3 (shown in green Figure 1b) were present in the lattice of **2**.

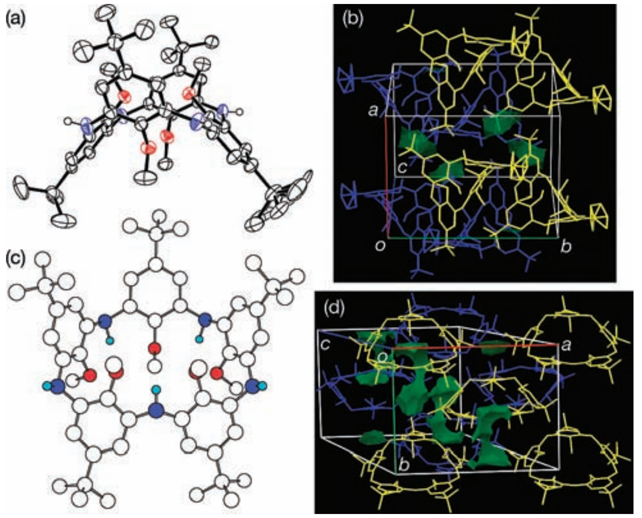

Figure 1. (a) ORTEP drawing[24] of **2**. The displacement ellipsoids are drawn at the 50% probability level. All hydrogen atoms except for the bridging NH atoms are omitted for clarity. One *tert*-butyl group is disordered over two positions. (b) Crystal structure of **2**. The molecules are shown by yellow and blue stick models, and the lattice voids are depicted as green Connolly surfaces (probe radius = 1.2 Å, grid = 0.2 Å). (c) Molecular structure of **3** in the solid state. All hydrogen atoms except for the bridging NH atoms are omitted for clarity. The carbon, nitrogen, oxygen, and hydrogen atoms are shown by white, blue, red, and sky blue circles, respectively. (d) Crystal structure of **3**. The molecules and the lattice voids are illustrated in the same manner as panel (b).

Despite our efforts, no single crystal growth occurred in the crystallization of **3** from a CH_2Cl_2/hexane mixture. Instead, a CH_2Cl_2 clathrate of **3** with a 1:2 host−guest ratio (Figures S7 and S8) was obtained as a crystalline powder. To solve the crystal structure of **3**, ab initio powder X-ray diffraction analysis (Figure S1) was performed for the desolvated powder (Figure S4) because the initially obtained CH_2Cl_2 clathrate slowly and spontaneously lost CH_2Cl_2 (Figure S8). The crystal structure of the solvent-free powder of **3**[19] was solved successfully by a direct-space approach[20] using the synchrotron X-ray diffraction

---

(7) (a) Pan, L.; Adams, K. M.; Herrandez, H. E.; Wang, X.; Zheng, C.; Hattori, Y.; Kaneko, K. *J. Am. Chem. Soc.* **2003**, *125*, 3062–3067. (b) Llewellyn, P. L.; Bourrelly, S.; Serre, C.; Filinchuk, Y.; Férey, G. *Angew. Chem., Int. Ed.* **2006**, *46*, 7751–7754. (c) Sung, J. W.; Jhung, S. H.; Hwang, Y. K.; Humphrey, S. M.; Wood, P. T.; Chang, J.-S. *Adv. Mater.* **2007**, *19*, 1830–1834. (d) Wang, B.; Côté, A. P.; Furukawa, H.; O'Keeffe, M.; Yaghi, O. M. *Nature* **2008**, *453*, 207–211. (e) Banerjee, R.; Furukawa, H.; Britt, D.; Knobler, C.; O'Keeffe, M.; Yaghi, O. M. *J. Am. Chem. Soc.* **2009**, *131*, 3875–3877. (f) Choi, H.-S.; Suh, M. P. *Angew. Chem., Int. Ed.* **2009**, *48*, 6865–6869.

(8) Furukawa, H.; Yaghi, O. M. *J. Am. Chem. Soc.* **2009**, *131*, 8875–8883.

(9) (a) Atwood, J. L.; Barbour, L. J.; Jerga, A. *Angew. Chem., Int. Ed.* **2004**, *43*, 2948–2950. (b) Thallapally, P. K.; Dobrzańska, L.; Gingrich, T. R.; Wirsig, T. B.; Barbour, L. J.; Atwood, J. L. *Angew. Chem., Int. Ed.* **2006**, *45*, 6506–6509. (c) Thallapally, P. K.; Dalgarno, S. J.; Atwood, J. L. *J. Am. Chem. Soc.* **2006**, *128*, 15060–15061. (d) Thallapally, P. K.; McGrail, B. P.; Atwood, J. L.; Gaeta, C.; Tedesco, C.; Neri, P. *Chem. Mater.* **2007**, *19*, 3355–3357. (e) Thallapally, P. K.; McGrail, B. P.; Dalgarno, S. J.; Schaef, H. T.; Tian, J.; Atwood, J. L. *Nat. Mater.* **2008**, *7*, 146–150.

(10) Tian, J.; Thallapally, P. K.; Dalgarno, S. J.; Atwood, J. L. *J. Am. Chem. Soc.* **2009**, *131*, 13216–13217.

(11) Dobrzańska, L.; Lloyd, G. O.; Raubenheimer, H. G.; Barbour, L. J. *J. Am. Chem. Soc.* **2006**, *128*, 698–699.

(12) Tozawa, T.; Jones, J. T. A.; Swamy, S. I.; Jiang, S.; Adams, D. J.; Shakespeare, S.; Clowes, R.; Bradshaw, D.; Hasell, T.; Chong, S. Y.; Tang, C.; Thompson, S.; Parker, J.; Trewin, A.; Bacsa, J.; Slawin, A. M. Z.; Steiner, A.; Cooper, A. I. *Nat. Mater.* **2009**, *8*, 973–978.

(13) Reviews on azacalixarenes: (a) Tsue, H.; Ishibashi, K.; Tamura, R. In *Heterocyclic Supramolecules I*; Matsumoto, K., Ed.; Topics in Heterocyclic Chemistry; Springer-Verlag: Berlin, Heidelberg, 2008; Vol. 17, pp 73−96. (b) Wang, M.-X. *Chem. Commun.* **2008**, 4541–4551. (c) Tsue, H.; Ishibashi, K.; Tamura, R. *J. Synth. Org. Chem. Jpn.* **2009**, *67*, 898–908.

(14) (a) Tsue, H.; Ishibashi, K.; Tokita, S.; Takahashi, H.; Matsui, K.; Tamura, R. *Chem.*−*Eur. J.* **2008**, *14*, 6125–6134. (b) Tsue, H.; Matsui, K.; Ishibashi, K.; Takahashi, H.; Tokita, S.; Ono, K.; Tamura, R. *J. Org. Chem.* **2008**, *73*, 7748–7755.

(15) Tsue, H.; Ishibashi, K.; Tokita, S.; Sakai, K. Japanese Patent Application No. 2009-21511.

(16) Crystal data for **2**: monoclinic, space group $P2_1/n$ (#14), a = 12.7494(7) Å, b = 16.1119(8) Å, c = 21.292(1) Å, β = 101.332(2)°, V = 4288.4(4) Å^3, Z = 4, ρ_{calc} = 1.098 g cm^{-3}, μ = 0.070 mm^{-1}, T = 296(2) K, 9812 independent reflections, 528 refined parameters, $R1$ = 0.0631 ($I > 2\sigma(I)$), $R1$ = 0.1252 (all reflections), $wR2$ = 0.2083, S = 1.085. CCDC-794847 contains the supplementary crystallographic data for this paper. The data can be obtained free of charge from The Cambridge Crystallographic Data Centre via www.ccdc.cam.ac.uk/data_request/cif.

(17) A detailed account of the crystal structures of **2** and **3** are given in the Supporting Information.

(18) Tsue, H.; Ishibashi, K.; Takahashi, H.; Tamura, R. *Org. Lett.* **2005**, *7*, 2165–2168.

data collected at the BL02B2 beamline[21] of the SPring-8. Azacalix[5]arene **3** adopts a 1,2-alternate conformation (Figure 1c) and forms a seemingly nonporous crystal structure[17] (Figures 1d and S10). Connolly surface analysis[22] indicates that the large lattice voids of 203 Å^3 (shown in green in Figure 1d) exist and are disconnected from each other. Accordingly, the crystal structure of **3** is not porous in the conventional sense and dictated as a seemingly nonporous crystal architecture,[23] which is much different from the one-dimensional (1D) channel structures established by **4** and **5**.[14]

Isothermal gas adsorption isotherms for four main atmospheric components such as N_2, O_2, Ar, and CO_2 were recorded at 293 K on **2** and **3** according to the described procedure.[25] As seen from Figure 2a and Table 1, azacalix[4]arene **2** (Figure S6) exhibited almost no uptake for all of the examined gases as observed in the *N*-methylated derivative **1**,[14a] indicating that the small lattice voids of 66 Å^3 of **2** were not enough to accommodate the gases. In contrast, the desolvated powder of azacalix[5]arene **3** with larger voids of 203 Å^3 selectively and rapidly adsorbed CO_2 at 293 K (Figure 2b), and the initial pressure of ca. 100 kPa was decreased within 20 min to reach equilibrium at 78 kPa, corresponding to the uptake of 11.5 mL of CO_2 per gram of **3** (Table 1). The adsorption capacity of **3** for CO_2 was lower than those of other materials such as MOF-5[26] and cucurbit[6]uril[4b] that adsorbed 47 and 45 mL g^{-1} of CO_2 under similar conditions, respectively. Nonetheless, it is worth noting that the CO_2 adsorption capacity of **3** exceeds the values of activated carbon and molecular sieve 5A examined herein as reference materials (Table 1). The molecules of CO_2 adsorbed on the crystalline powder of **3** were desorbed by applying a reduced pressure, and the adsorption and desorption of CO_2 could be repeated with reproducibility, as shown in Figure S12. The high selectivity of **3** for CO_2 was also operative in another gas adsorption experiment using a gas mixture of $N_2/CO_2 = 9:1$ (v/v) which was used as a model flue gas (Figure 2c and 2d). After the solvent-free powder of **3** (37.5 mg) was allowed to stand in the gas (2.5 mL) at 293 K for 30 min, no CO_2 was detected in the gas chromatographic analysis, as shown in Figure 2d.

Table 1. Gas Adsorption Capacities (mL g^{-1}) of Azacalixarenes, Activated Carbon, and Molecular Sieve 5A for N_2, O_2, Ar, and CO_2 at 293 K

adsorbent	gas adsorption capacity/mL g^{-1}			
	N_2	O_2	Ar	CO_2
1[a]	<0.1	<0.1	<0.1	<0.1
2	<0.1	<0.1	<0.1	0.2
3	1.8	1.6	1.8	11.5
4[a]	0.6	0.3	0.2	2.3
5[b]	0.9	0.9	0.9	3.0
activated carbon[c]	1.5	1.5	1.9	9.2
molecular sieve 5A[d]	1.5	1.1	1.6	7.1

[a] Reference 14a. [b] Reference 14b. [c] Wako Pure Chemical, Lot No. WDP1201. [d] Wako Pure Chemical, Lot No. SAQ3823.

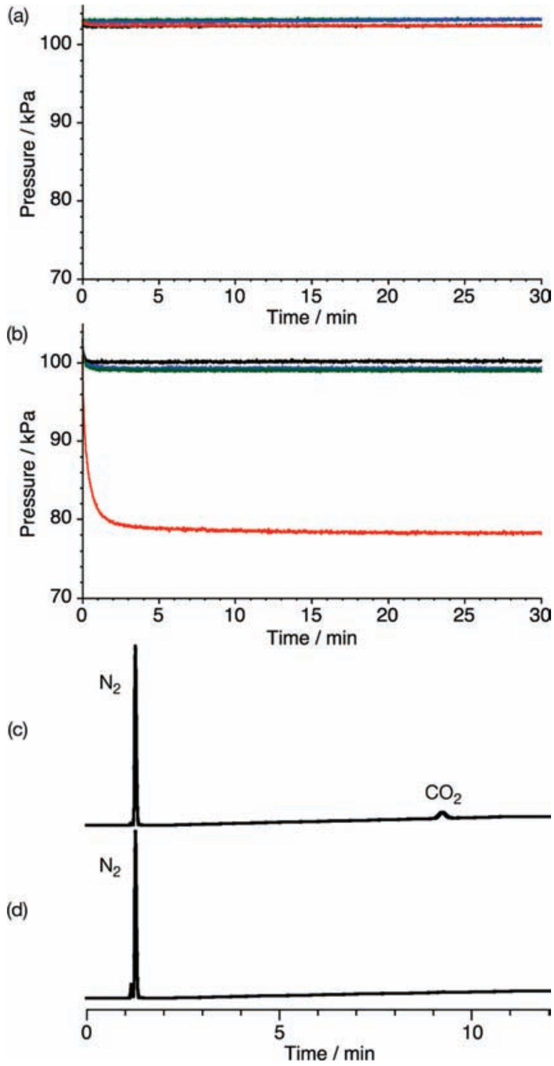

Figure 2. Isothermal gas adsorption isotherms recorded at 293 K for N_2, O_2, Ar, and CO_2 using (a) **2** and (b) **3** as adsorbents. Isotherms for N_2, O_2, Ar, and CO_2 are shown by green, black, blue, and red lines, respectively. Gas chromatograms (c) before and (d) after the gas adsorption experiments at 293 K using **3** as a adsorbent and $N_2/CO_2 = 9:1$ (v/v) as a gas mixture.

To understand the observed selective CO_2 uptake in azacalix[5]arene **3** under ambient conditions, potential energy distribution analysis based on the Lennard−Jones potential was performed and led to the conclusion that the lattice voids

---

(19) Crystal data for **3**: monoclinic, space group $P2_1/c$ (#14), $a = 17.11(1)$ Å, $b = 13.11(1)$ Å, $c = 26.90(2)$ Å, $\beta = 109.374(2)°$, $V = 5690.7$ Å^3, $Z = 4$, $\rho_{calc} = 1.034$ g cm^{-3}, $T = 293(2)$ K, $R_p = 0.050$, $R_{wp} = 0.074$.

(20) (a) Harris, K. D. M.; Tremayne, M.; Kariuki, B. M. *Angew. Chem., Int. Ed.* **2001**, *40*, 1626–1651. (b) Tsue, H.; Horiguchi, M.; Tamura, R.; Fujii, K.; Uekusa, H. *J. Synth. Org. Chem. Jpn.* **2007**, *65*, 1203–1212.

(21) Nishibori, E.; Takata, M.; Kato, K.; Sakata, M.; Kubota, Y.; Aoyagi, S.; Kuroiwa, Y.; Yamakata, M.; Ikeda, N. *J. Phys. Chem. Solids* **2001**, *62*, 2095–2098.

(22) Mercury CSD, version 2.3; The Cambridge Crystallographic Data Centre: Cambridge, U.K., 2009.

(23) Barbour, L. J. *Chem. Commun.* **2006**, 1163–1168.

(24) Farrugia, L. J. *J. Appl. Crystallogr.* **1997**, *30*, 565.

(25) Atwood, J. L.; Barbour, L. J.; Thallapally, P. K.; Wirsig, T. B. *Chem. Commun.* **2005**, 51–53.

(26) Lu, C.-M.; Liu, J.; Xiao, K.; Harris, A. T. *Chem. Eng. J.* **2010**, *156*, 465–470.

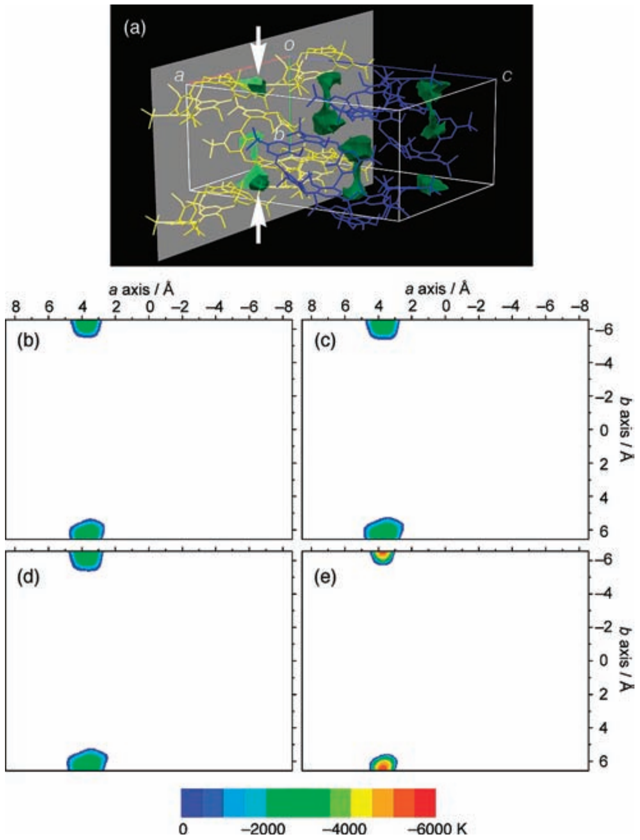

Figure 3. (a) Crystal structure of **3**. The molecules and the lattice voids are illustrated in the same manner as Figure 1b. The (005) plane is shown in gray, and the lattice voids on the plane are marked by white arrows. Panels (b), (c), (d), and (e) indicate the potential energy contour maps on the (005) plane for N_2, O_2, Ar, and CO_2, respectively.

of **3** created an energetically favorable space particularly for CO_2, as shown in Figure 3. The large potential energy for CO_2 would be ascribed to the dispersion force and the dipole/quadrupole interaction between **3** and CO_2, judging from the larger polarizability of CO_2 (2.93×10^{-40} C m^2 J^{-1}) compared to N_2 (1.97×10^{-40}), O_2 (1.78×10^{-40}), and Ar (1.81×10^{-40}) and from the larger quadrupole moment (absolute value)[27] of CO_2 (13.4×10^{40} C m^2) compared to N_2 (4.7×10^{40}), O_2 (1.3×10^{40}), and Ar (0). Although the crystal structure of **3** is seemingly nonporous, thermal motion would create a transient "window" welcoming the molecules of CO_2, which would penetrate and diffuse into the crystal owing to its small kinetic diameter (3.3 Å)[28] compared to the other gases such as N_2 (3.64 Å), O_2 (3.46 Å), and Ar (3.40 Å). The same analysis was carried out for azacalix[7]-arene **5** which adsorbed 3.0 mL g^{-1} of CO_2 at 293 K (Table 1).[14b] As shown in Figure S11, potential energy distribution analysis of **5** indicated that stabilization in the open 1D channel of **5** was, on the whole, smaller than that of **3**, thus preventing the efficient CO_2 uptake of **5** at ambient conditions. In other words, it is conceivable that once the smallest CO_2 molecule permeates the crystal of **3** and then reaches the lattice voids, the molecule is exposed to large van der Waals interactions probably as well as hydrogen bonding interactions, thereby leading to the observed selective CO_2 adsorption on **3** under ambient temperature and pressure.

In conclusion, we have demonstrated that azacalix[5]arene **3** forms a seemingly nonporous crystal, which adsorbs CO_2 selectively and rapidly under ambient conditions. We should emphasize that the CO_2 adsorption capacity of **3** under such conditions exceeds the capacities of the larger homologues **4** and **5** and of conventional adsorbents such as activated carbon and molecular sieve 5A. X-ray crystallographic and potential energy distribution analysis clearly revealed that crystal architecture defined the potential energy in the crystal and hence controlled the solid−gas adsorption behavior. Accordingly, we anticipate that crystal engineering and functionalization of the present molecular system lead to a more efficient uptake of CO_2. Investigations along this line are currently in progress in our laboratory.

Acknowledgment. This work was supported by the ENEOS Hydrogen Trust Fund. Synchrotron radiation experiments were performed at the BL02B2 beamline of the SPring-8 with the approval of the Japan Synchrotron Radiation Research Institute (JASRI) (Proposal Nos. 2009A1425, 2010A1346, and 2010B1496).

Supporting Information Available: Syntheses, experimental procedures, characterization data, NMR spectra and crystal structures of **2** and **3**, synchrotron powder XRD pattern of **2**, ^{1}H NMR spectrum and TGA thermogram of the CH_2Cl_2 clathrate of **3**, and potential energy distribution analysis of **5**. This material is available free of charge via the Internet at http://pubs.acs.org.

OL102829H

---

(27) Steele, W. *Chem. Rev.* **1993**, *93*, 2355–2378.

(28) Breck, D. W. *Zeolite Molecular Sieves*; John Wiley & Sons: New York, 1974; pp 633−645.